THE ASTROPHYSICAL JOURNAL, 438:72–82, 1995 January 1


# THE MASS-TO-LIGHT RATIOS OF LOW SURFACE BRIGHTNESS SPIRAL GALAXIES: CLUES FROM THE TULLY-FISHER RELATION

D. SPRAYBERRY,[1,2] G. M. BERNSTEIN,[2,3] AND C. D. IMPEY[1,2]
Steward Observatory, University of Arizona, Tucson, AZ 85721;
dsprayberry@as.arizona.edu; gbernstein@as.arizona.edu; cimpey@as.arizona.edu

AND

G. D. BOTHUN[1]
Department of Physics, University of Oregon, Eugene, OR 97403; nuts@moo.uoregon.edu
*Received 1994 April 28; accepted 1994 July 7*

## ABSTRACT

We have obtained 21 cm profiles and CCD surface photometry for a subset of field low surface brightness (LSB) spiral galaxies found by a large survey using the Automated Plate Measuring machine. We find that the LSB spirals generally follow the same Tully-Fisher relations defined by a sample of higher surface brightness (HSB) galaxies drawn from the Ursa Major cluster, albeit with a considerably greater scatter. This general trend implies that LSB galaxies of a given total luminosity have mass-to-light ratios ($M/L$) similar to those of HSB galaxies of comparable total luminosity, despite their differences in luminosity density (i.e., surface brightness). We also find evidence that galaxies with extremely large half-light radii (the "Malin 1 cousins") tend to be excessively luminous for their rotation speeds. We find that, at a given profile width, the luminosity of an LSB galaxy relative to the Tully-Fisher relation seems to be weakly anticorrelated with gas richness, indicating that some of the higher scatter may be associated with the evolutionary status of the LSB galaxies. Finally, we find that the LSB galaxies tend to have higher total atomic gas masses than the Ursa Major comparison galaxies, despite the generally comparable optical luminosities between the two sets.

*Subject headings:* galaxies: fundamental parameters — galaxies: photometry — galaxies: spiral — radio lines: galaxies

## 1. INTRODUCTION

The night sky, by virtue of its intrinsic brightness and its color, forms a powerful filter through which we must look when we study the universe. This filter clearly constrains our knowledge of the properties of galaxies: as Disney (1976) described, it defines a "visibility" function which, when convolved with the true population of galaxies, yields the populations recorded in the standard galaxy catalogs. The night sky thus has significant effects on our knowledge of galaxy properties, but the severity of those effects has only recently become the subject of quantitative study.

The first step in studying these effects is simply to identify galaxies that have been previously missed because of their low contrast against the night sky. The first such efforts were made in studies of galaxy clusters, particularly the Virgo and Fornax Clusters. The massive study of the Virgo Cluster by Binggeli, Sandage, & Tammann (1985) was the first to note the presence of a significant number of very low surface brightness (LSB) galaxies. Subsequently, Impey, Bothun, & Malin (1988) (Virgo Cluster), Irwin et al. (1990) (Fornax Cluster), and Bothun, Impey, & Malin (1991) (Fornax Cluster) identified more galaxies at even lower surface brightness levels. In addition to these cluster studies, several field surveys for LSB galaxies are underway. Schombert & Bothun (1988) and Schombert et al. (1992) visually searched POSS-II survey plates to identify several hundred new LSB galaxies in the northern sky. Impey et al. (1994) have used APM machine scans of UK Schmidt Telescope survey plates to identify over 500 new LSB galaxies around the celestial equator. Finally, Miller & MacGillivray (1994) have a survey of the southern sky still underway, using the COSMOS machine at Royal Observatory in Edinburgh to scan ESO/SERC survey plates; they project a final catalog of about 7000 LSB galaxies. The numbers of LSB galaxies found in these surveys underscores the severity of the selection effect imposed by the sky brightness on existing catalogs.

The next step in determining the pernicious effects of sky brightness is to compare the properties of LSB galaxies to those of HSB galaxies. One particularly interesting galaxian property is the mass-to-light ratio ($M/L$). For example, it is important to know whether LSB galaxies represent a cosmologically significant amount of baryonic matter that has been overlooked by previous galaxy surveys. Since determination of the masses of large numbers of individual galaxies is difficult, it makes more sense to proceed by determining a luminosity function for LSB galaxies, and then in some way estimating their $M/L$ to arrive at a mass distribution function. Also, comparisons of the $M/L$ of LSB and HSB galaxies could help shed light on the reasons for their apparent differences in stellar populations and evolution as noted by McGaugh & Bothun (1994). Although Impey et al. (1988) and Bothun et al. (1991) were unable to quantify the $M/L$s for the LSB dwarf galaxies of the Virgo or Fornax Clusters, they concluded that these small ($-11 \lesssim M_B \lesssim -15.5$) galaxies must have very high $M/L$s in order to survive the tidal fields of those massive clusters. If LSB is correlated with high $M/L$, then the more luminous LSB spirals in the general field could have very high total masses. In

[1] Visiting Scientist, Arecibo Observatory. The Arecibo Observatory is part of the National Astronomy and Ionosphere Center, which is operated by Cornell University under a cooperative agreement with the National Science Foundation.

[2] Optical observations were made with the Steward Observatory 2.3 m telescope located on Kitt Peak.

[3] Bart J. Bok Fellow.

order to address this question, we have studied such a set of field LSB spiral galaxies ($-17.5 \lesssim M_B \lesssim -21.5$) to see how their $M/L$s compare to those of HSB galaxies having similar total luminosities.

Actually determining a $M/L$ for any individual spiral galaxy requires a well-measured rotation curve and a halo with several assumed parameters, as exemplified by the work of Kent (1986, 1987). However, it is possible to compare $M/L$s at a particular radius for two different sets of spiral galaxies by comparing their locations in the luminosity–H I profile width plane. HSB spiral galaxies fall along a well-defined track in this plane: the famous Tully-Fisher relation, from Tully & Fisher (1977). The virial theorem for a galaxy bound by Newtonian gravity gives $M/r \propto v^2$, where $r$ is the galactocentric radius, $v$ is the rotation speed at that radius, and $M$ is the mass enclosed within that radius. Taking $\langle\mu\rangle$ as the mean surface brightness, we have the luminosity as $L \propto \langle\mu\rangle r^2$. Assuming $\langle\mu\rangle$ and $M/L$ are constant, the relation $L \propto v^4$ can be readily obtained. Thus, under these idealized assumptions, the Tully-Fisher relation should have a slope of 10. Variations in $M/L$ among individual galaxies in the set will produce scatter around this slope. Any dependence of $M/L$ on $L$, or of $\langle\mu\rangle$ on $L$, will change the slope. If two samples of galaxies have systematically different $M/L$s, this difference will manifest itself as an offset in their Tully-Fisher zero points. Bothun & Mould (1987) showed that surface brightness variations within a fixed profile width can contribute greatly to the scatter around the Tully-Fisher relation. They were attempting to improve the Tully-Fisher relation as a distance indicator, and they found that the scatter in the relation could be reduced significantly by excluding the galaxies with the highest and lowest overall surface brightness. We take the opposite approach here; we intend to use the deviations from a baseline Tully-Fisher relation to learn something about other properties of the LSB glaxies.

To that end, we present photometric and 21 cm radio observations of a sample of LSB galaxies. In § 2 we describe the galaxies chosen for this comparison and the data reduction and analysis techniques employed. Section 3 contains the comparison of LSB and HSB Tully-Fisher relations, and in § 4 we review the implications of those comparisons for both the LSB galaxies and the Tully-Fisher relation itself. Section 5 lists our conclusions.

## 2. DATA REDUCTION AND ANALYSIS

### 2.1. *Galaxy Selection and Data Reduction*

We have chosen galaxies for this study from the survey of Impey et al. (1994), who give a complete description of the survey parameters. The sample of galaxies is complete to specific angular size and surface brightness criteria: machine scanning verifies that all objects with an average surface brightness of $\mu_B \geq 23$ mag arcsec$^{-2}$ within the 25 mag arcsec$^{-2}$ isophote and with an angular size in the range $13'' \leq D_{25} \leq 200''$ (where $D_{25}$ is the diameter at an effective surface brightness of 25 mag arcsec$^{-2}$) will be found. CCD images were also obtained in $B$, $V$, and $R$ of over 100 of the LSB galaxies found by that survey, and almost 200 of the galaxies were detected in the 21 cm H I line with the 305 m Arecibo telescope. We have chosen from that database all the spiral galaxies that have H I profile widths $W_{50} > 180$ km s$^{-1}$ (where $W_{50}$ is the width measured at 50% of the mean flux) and that have CCD images. We also independently obtained CCD images in $I$ of 11 of LSB galaxies which met all of the above criteria, seven of which also had $BVR$ photometry. Finally, after measuring the ellipticities as described below, we further eliminated those galaxies with ellipticities $e < 0.3$ (i.e., inclinations $i \lesssim 45°$). Small inclination angles require large $1/\sin i$ corrections to obtain the edge-on profile width from the observed profile width, and the large corrections raise the uncertainties in the profile widths to unacceptable levels. The final sample of LSB galaxies includes 21 galaxies measured in $B$, 17 galaxies measured in $R$, and 10 galaxies measured in $I$.

The CCD images were bias-subtracted and flat-fielded using standard IRAF tasks. Total integrated magnitudes were then determined for all galaxies using modified VISTA routines. First, sky values and uncertainties were measured using the corners of the image or four other large regions well away from the galaxy. Second, the sky was subtracted from the image as a constant or as a flat plane if there was a smooth gradient in the sky across the image. Third, elliptical isophotes were fitted to the galaxy image. Fourth, a two-dimensional radial profile of averaged isophotal surface brightness versus isophotal semimajor axis was plotted, and an exponential model was fitted to regions of the radial profile that appeared to be well beyond any bulge or central condensation. Also, at this point both the radial surface brightness profile and the radial total intensity growth curve were examined for evidence of errors in the sky level; if any were suspected, the entire process was repeated with an adjusted sky level. Fifth, the total Galactic intensity (i.e., including both bulge and disk) was determined by summing the actual pixel intensities inside the outermost isophote, and then extrapolating the exponential fit only from this last isophote to infinity. This extrapolation typically increased the galactic magnitude by less than 0.1 mag. Finally, this total intensity was transformed to a total magnitude in the usual manner using zero points and color terms derived from observations of standard stars from Landolt (1992), Christian et al. (1985), and Odewahn, Bryja, & Humphreys (1992). We corrected for Galactic reddening using the maps of Burstein & Heiles (1982), and applied $k$-corrections from the tabulations of Coleman, Wu, & Weedman (1980). For those galaxies observed in more than one filter, the isophotes were fitted only to one filter, and the same isophotes were used as elliptical apertures for summing intensities in the other filters. This procedure ensures that both the radial color profiles and the total colors of the galaxies are uniformly measured.

A brief comment about the colors is necessary here. For those galaxies with both $B$ and $R$ magnitudes, the $B-R$ colors are fairly reliable, in that $B$, $V$, and $R$ images were obtained on the same nights and processed and calibrated in parallel. The $I$ images, and the $B$ images of the four galaxies that do not also have $R$ data, were all obtained some months later using different CCDs, different filters, different standard stars, and different observing techniques. Hence the $B-I$ and $R-I$ colors are probably not as trustworthy. Galaxy 0233+0012 illustrates the problem. Its colors are $B-R = 1.13$ and $R-I = -0.41$. Much of this inconsistency in color is probably due to a difference in observing techniques. The $B$, $V$, and $R$ images were taken as single long exposures centered on the galactic nucleus with a TI $800^2$ pixel CCD that could be flat-fielded well with dark sky flats. The $I$-band image was taken with a Loral $800 \times 1200$ pixel CCD which has the same pixel scale as the TI but also has severe fringing at long wavelengths. The $I$ image was compiled from a series of short exposures, each taken with the galaxy in a different part of the field of view. This procedure allowed better flat-fielding, but resulted in a small composite

image that has few if any sky pixels that are not contaminated at some level by the faint outer regions of the galactic disk. Thus the $I$ luminosity for this object is probably underestimated due to the likely overestimation of the sky flux level.

For each galaxy, a disk ellipticity was estimated by a simple average of the ellipticities of all the isophotes used in fitting the exponential disk profile. The inclination was determined by assuming that the ellipticity was due to the inclination of a circular disk, and that an edge-on disk would have an intrinsic ellipticity of 0.8, per Holmberg (1958). Finally, a half-light radius was measured for each galaxy by locating the semimajor axis at which the integrated magnitude was 0.753 mag fainter than the extrapolated total magnitude. We have chosen to report this half-light radius, rather than the fitted disk exponential scale length, because it is model-independent, and because it reflects to some extent the degree of central condensation in the luminosity profile, as well as the scale of the disk.

H I parameters of these galaxies were determined from 21 cm observations using the Arecibo radio telescope. The data were reduced on-site using the Arecibo Observatory's standard GALPAC software. Widths of the reduced H I profiles were measured in several different ways; those shown here are $W_{50}$, the full width at 50% of the mean flux across the profile, and $W_{20}$, the full width at 20% of the peak flux. Heliocentric radial velocities were determined from the centers of the profiles and adjusted for Galactic rotation using the conventional 300 sin $l$ cos $b$ km s$^{-1}$ correction. The reduced data values for the selected LSB galaxies appear in Table 1.

### 2.2. *Selection of HSB Comparison Sets*

The desiderata for a comparison set of HSB galaxies are fairly simple. First, the chosen set must have H I and photometric data comparable to those of our LSB set. In particular, the galactic magnitudes should be determined by surface photometry rather than aperture photometry, to ensure that the galaxy magnitudes are measured in a way that does not introduce a bias toward underestimating luminosity as galaxy scale length increases, as detailed in Bothun & Mould (1987). Second, the comparison galaxies should cover ranges of luminosity and H I profile width comparable to those covered by the LSB galaxies, to ensure that any effects seen are caused by the surface brightness difference and not by differences in total luminosity or mass. Finally, it would be helpful to have some color information available for the comparison set, to see if any observed differences in the Tully-Fisher relation can be related to possible differences in stellar populations.

The Ursa Major Cluster of galaxies satisfies this bill of particulars nicely. The magnitudes reported by Pierce & Tully (1988) are derived from surface photometry, and comparable color information is available. Both samples cover a similar range of Tully-Fisher parameters, and the Ursa Major cluster has no special problems of internal structure or projection effects. Pierce & Tully (1988) used isophotal magnitudes within the outermost fitted isophote without adding an extrapolation of the disk model as we did for our LSB set. This extrapolation increased the uncertainties in our total magnitudes slightly as compared with the isophotal magnitudes. However, for two galaxies of equal total luminosity, the one with the lower central surface brightness will have a larger fraction of its total light outside of any given isophotal level. Use of the extrapolated totals avoided this source of possible bias and justified the larger random uncertainties. We have included the uncertainties associated with the extrapolation in our estimates of the total photometric uncertainties (see § 3.3).

TABLE 1

LOW SURFACE BRIGHTNESS GALAXIES

| Name | RA[a] (h m s) | Dec[a] (° ′ ″) | $v$[b] (km/s) | $W_{50}$[c] (km/s) | $W_{20}$[d] (km/s) | $e$[e] | $R_{1/2}$[f] (kpc) | $B_T$ (mag) | $R_T$ (mag) | $I_T$ (mag) |
|---|---|---|---|---|---|---|---|---|---|---|
| 0014+0115 | 0:14:03.1 | +1:15:23 | 12377 | 233 | 250 | 0.34 | 6.1 | 15.91 | 14.98 | ... |
| 0023+0044 | 0:23:51.1 | +0:44:35 | 5502 | 318 | 333 | 0.39 | 5.2 | 16.02 | 15.05 | 14.56 |
| 0050+0230 | 0:50:54.4 | +2:30:11 | 5126 | 226 | 230 | 0.39 | 2.8 | 15.62 | 14.66 | ... |
| 0059+0248 | 0:59:11.4 | +2:48:47 | 4499 | 178 | 187 | 0.54 | 4.0 | 15.77 | 15.21 | 14.84 |
| 0142−0033 | 1:42:29.8 | −0:33:06 | 5480 | 165 | 179 | 0.32 | 3.5 | 16.89 | 16.00 | ... |
| 0229+0004 | 2:29:09.4 | +0:04:22 | 6369 | 212 | 224 | 0.46 | 5.4 | 15.60 | 14.72 | 14.39 |
| 0233+0012 | 2:33:26.9 | +0:12:10 | 2648 | 194 | 201 | 0.40 | 4.7 | 14.19 | 13.06 | 13.47 |
| 0243+0301 | 2:43:13.1 | +3:01:13 | 6846 | 339 | 345 | 0.61 | 4.5 | 15.17 | 14.42 | ... |
| 0400+0149 | 4:00:12.6 | +1:49:36 | 3781 | 493 | 499 | 0.75 | 7.2 | 14.09 | ... | 11.40 |
| 0411+0236 | 4:11:46.8 | +2:36:21 | 3293 | 270 | 270 | 0.50 | 4.3 | 14.62 | ... | 12.91 |
| 0918−0028 | 9:18:03.9 | −0:28:01 | 3290 | 277 | 329 | 0.35 | 1.8 | 15.60 | 14.49 | ... |
| 1106+0032 | 11:06:06.2 | +0:32:16 | 7466 | 334 | 338 | 0.43 | 4.3 | 16.12 | 15.03 | ... |
| 1132+0249 | 11:32:30.9 | +2:49:40 | 5088 | 182 | 196 | 0.70 | 4.6 | 15.58 | 14.88 | ... |
| 1209+0137 | 12:09:25.9 | +1:37:40 | 6136 | 275 | 292 | 0.43 | 3.2 | 16.02 | 15.11 | ... |
| 1226+0105 | 12:26:39.2 | +1:05:39 | 23529 | 269 | 278 | 0.32 | 15.7 | 16.10 | 15.01 | ... |
| 1300+0144 | 13:00:42.6 | +1:44:12 | 12164 | 393 | 393 | 0.74 | 9.9 | 17.42 | 15.94 | ... |
| 2303−0006 | 23:03:57.8 | −0:06:02 | 7644 | 295 | 303 | 0.41 | 6.3 | 14.41 | 13.57 | 13.14 |
| 2315−0000 | 23:15:41.9 | −0:00:43 | 9109 | 420 | 428 | 0.40 | 9.2 | 15.19 | ... | 13.16 |
| 2318+0236 | 23:18:34.0 | +2:36:35 | 4112 | 217 | 229 | 0.36 | 2.9 | 15.64 | ... | 14.20 |
| 2344+0139 | 23:44:47.4 | +1:39:20 | 5397 | 197 | 205 | 0.37 | 4.2 | 15.14 | 13.90 | ... |
| 2349+0248 | 23:49:17.0 | +2:48:14 | 5489 | 280 | 290 | 0.37 | 6.3 | 14.39 | 13.68 | 13.15 |

[a] All coordinates are for the 1950.0 equinox.
[b] Radial velocity in km s$^{-1}$, corrected for Local Group motion as described in the text.
[c] Full width of 21 cm profile in km s$^{-1}$, measured at 50% of the mean flux across the profile.
[d] Full width of 21 cm profile in km s$^{-1}$, measured at 20% of the peak flux in the profile.
[e] Ellipticity = $(1 - b/a)$, measured as described in the text.
[f] Half-light radius in kiloparsecs, assuming $H_0 = 100$ km s$^{-1}$ Mpc$^{-1}$.

The Coma Cluster sample of Bernstein et al. (1994) was also used; indeed, the comparison with this Coma sample was what first inspired this study. However, the Coma sample fails to meet two of the criteria: Bernstein et al. (1994) obtained only *I* magnitudes, and their sample covers different ranges in both H I profile width and luminosity. *B* magnitudes for most of the Coma sample were reported by Fukugita et al. (1991), but those magnitudes were measured from photographic plates, so the color information is not as precise as for the other samples. To ensure consistency with the LSB sample, we also removed from the Ursa Major sample of Pierce & Tully (1988) three galaxies with $i < 45°$, leaving 23 galaxies in that sample. Bernstein et al. (1994) used the same minimum ellipticity of 0.3 for their sample of Coma galaxies, so we eliminated none from the Coma set, which includes 17 galaxies in *B* and 18 galaxies in *I*. The profile widths and magnitudes of the comparison sets were used as reported by Pierce & Tully (1988) for Ursa Major and Bernstein et al. (1994) for Coma. Because these two groups used different adjustments to account for the effects of inclination on profile width and magnitude, it was necessary to adjust the data for the LSB galaxies separately for each comparison.

In adjusting the LSB data for comparison to the Ursa Major set, we followed the system used by Pierce & Tully (1988) who had in turn adopted adjustments proposed by Tully & Fouqué (1985). First, we obtained the "rotational profile width" $W_r$ from the measurement of $W_{20} = W_{20}^{\rm raw}/(1+z)$ as

$$W_r^2 = W_{20}^2 + W_t^2 - 2W_{20}W_t(1-e^{-\alpha}) - 2W_t^2 e^{-\alpha}, \quad (1)$$

where $W_t$ is the velocity component due to random thermal motions, $\alpha = (W_{20}/W_c)^2$, and $W_c$ is a scaling parameter chosen to provide a smooth transition between a linear summation of the rotation and dispersion terms (for giant galaxies) and quadrature summation (for dwarf galaxies). For consistency with Tully & Fouqué (1985) and Pierce & Tully (1988), we adopted $W_t = 38$ km s$^{-1}$ and $W_c = 120$ km s$^{-1}$. Given the profile width constraint applied in the selection of LSB galaxies for this study, this fomula closely approximates a linear subtraction of 38 km s$^{-1}$. This rotational width $W_r$ is set to its edge-on value as $W_{rc} = W_r/\sin i$. We note that equation (1) may not be applicable to LSB galaxies; in systems with lower surface mass density, the restoring force is reduced and deviations from circular motion are likely to be more prominent than assumed in equation (1). We emphasize that we are applying equation (1) here solely for consistency of treatment with Pierce & Tully (1988). Second, galaxy total magnitudes in *B* were corrected to face-on values by subtracting the net internal extinction due to inclination $A_B^{i-0} = A_B^i - A_B^0$. $A_B^i$ is found by

$$A_B^i = -2.5\log\left[f(1+e^{-\tau\sec i}) + (1-2f)\left(\frac{1-e^{-\tau\sec i}}{\tau\sec i}\right)\right], \quad (2)$$

where $\tau = 0.55$ is the assumed optical depth and $f = 0.25$ is the unobscured fraction of the disk facing the observer, and $A_B^0 = 0.27$ from the preceding equation with $i = 0$. For consistency with Pierce & Tully (1988), we assumed that extinctions in *R* and *I* were 61% and 44% of that in *B*. Finally, to make the inclination-corrected apparent magnitudes directly comparable to those for the Ursa Major set, we adjusted the LSB galaxy magnitudes by 5 log ($v$/1324), where $v$ is the LSB galaxy's radial velocity from Table 1 and 1324 km s$^{-1}$ is the systemic velocity of the Ursa Major cluster given by Pierce & Tully (1988).

In adjusting the LSB data for comparison to the Coma set, we followed the procedures outlined by Bernstein et al. (1994). The inclination-corrected (i.e., edge-on) profile width was determined simply as $W_c = W_{50}^{\rm raw}/[(1+z)\sin i]$. Internal extinction corrections to the *I* apparent magnitudes followed the empirical scaling derived from the Coma comparison set of $\Delta I = 1.4e$, where $e$ is the ellipticity. We derived an internal extinction correction in *B* of $\Delta B = 1.9e$ by applying the same empirical method of Bernstein et al. (1994) to the Coma galaxies' *B* magnitudes reported by Fukugita et al. (1991). That method involves fitting a Tully-Fisher relation to the uncorrected magnitudes, plotting the residuals from that relation as a function of ellipticity, then fitting a straight line to that plot and using the slope of the line as the correction factor. Again, we applied these extinction corrections determined from the Coma galaxies to the LSB sample solely to ensure consistency of treatment with Bernstein et al. (1994). Finally, the inclination-corrected apparent magnitudes of the LSB galaxies were adjusted by 5 log ($v$/7000) to achieve the same zero point as the Coma galaxies.

## 3. COMPARISON OF TULLY-FISHER RELATIONS

### 3.1. *Luminosity–Profile Width Correlations*

Figure 1 shows the comparison of the Ursa Major and LSB Tully-Fisher relations in *B*, *R*, and *I*, and Figure 2 shows the comparison of the Coma and LSB Tully-Fisher relations. The LSB galaxies are clearly less tightly correlated than either the Ursa Major or Coma galaxies. Coefficients of the correlation between luminosity and profile width for the various samples are given in Table 2; coefficients are shown for both parametric linear correlation and nonparametric Spearman rank correlation. The coefficients for the LSB galaxies are reported both for the full sample and (in *B* and *R*) after excluding the galaxies with the largest and smallest half-light radii (the "restricted sample"). In the *I* band, the null hypothesis that the correlations of the LSB and Ursa Major galaxies are the same can be rejected at the 96% confidence level; in the other wavebands, this null hypothesis can be rejected at confidence levels greater than 99%. For the LSB galaxies, the luminosity-profile width correlation is stronger in *I* than in *B* or *R*, but the differences are not highly significant, in the sense that the null hypothesis that the correlations are the same can be rejected at only about the 80% confidence level for the complete LSB sample, or about the 90% confidence level for the restricted LSB sample. The reduction of scatter in the Tully-Fisher relation with increasing wavelength has been noted before, beginning with Aaronson, Huchra, & Mould (1979), and is usually taken as indicating that shorter wavelengths are more strongly affected by internal extinction and the luminosity of bright but relatively scarce young stars.

### 3.2. *Slopes of the Luminosity–Profile Width Relations*

Table 3 shows the fit parameters for the luminosity-profile width relations of the various samples. The entries designated "forward" are the results of standard least-squares fits which treat profile width as the independent variable and minimize the residuals in luminosity. The entries designated "double" are the results of double-regression fitting which simultaneously minimizes residuals in both luminosity and profile width. Because the profile width has large relative measurement uncertainties, these uncertainties dominate the weighting in these fits and cause the results to closely resemble those of a "reverse" fit (i.e., one where luminosity is the independent variable and profile width is the dependent variable). Two fits are

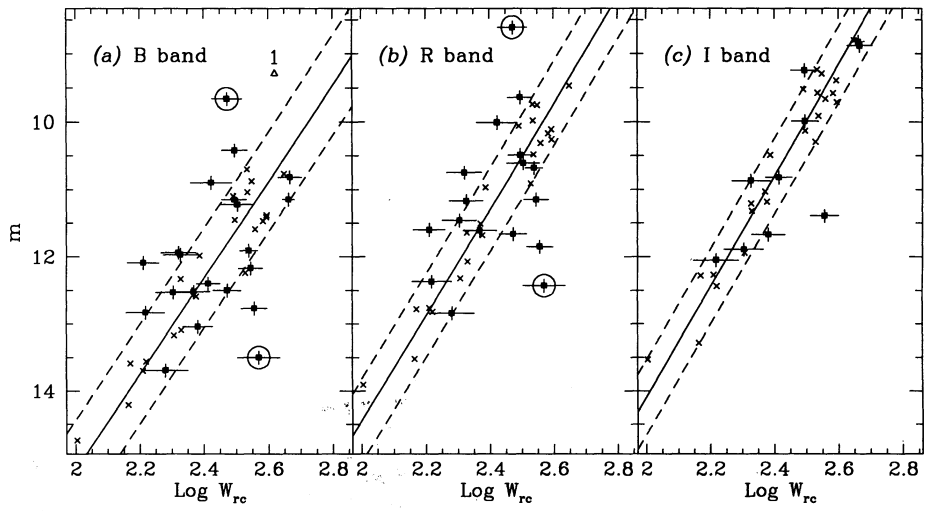


FIG. 1.—Tully-Fisher relations in *B*, *R*, and *I*. Filled squares represent the LSB spirals, and crosses represent the Ursa Major comparison galaxies. Solid lines are double-regression fits to the Ursa Major galaxies, and dashed lines show the 2 $\sigma$ range around those fits. The labeled triangle shows the position of Malin 1. Open circles mark the LSB galaxies excluded from the "restricted" sample because of their radii.

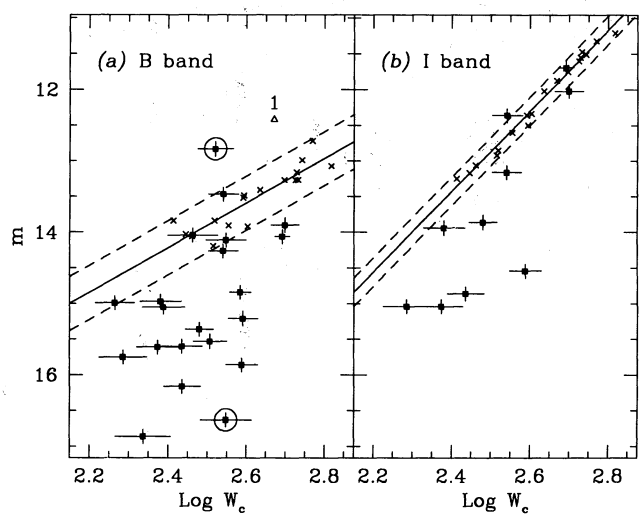


FIG. 2.—Tully-Fisher relations in *B* and *I* for the LSB spirals (*filled squares*) and the Coma comparison galaxies (*crosses*). Solid lines show the forward fit to the Coma galaxies, and the dashed lines show the 2 $\sigma$ range around that fit. Coma *I* data and fit are from Bernstein et al. (1994). Coma *B* magnitudes are those reported by Fukugita et al. (1991) for the same galaxies covered by Bernstein et al. (1994). The triangle shows the position of Malin 1. Open circles mark the LSB galaxies excluded from the "restricted" sample because of their radii.

reported for the Ursa Major sample; these are the forward and double-regression fits obtained by us on the sample without the three galaxies with $i < 45°$. The exclusion of these three galaxies changed the double-regression slope from the value reported by Pierce & Tully (1988) by an amount smaller than the error bars on either fit.

The forward and double-regression fit parameters for the LSB galaxies bracket the parameters for the Ursa Major comparison set, and the differences in all cases are larger than the formal errors. To test the significance of these differences, a reduced $\chi^2_\nu$ was calculated as a measure of goodness of fit to the LSB galaxies for each of the lines fitted to the LSB galaxies and to the Ursa Major galaxies. *F* tests were applied with the null hypothesis that the reduced $\chi^2_\nu$'s are indistinguishable. In all cases and in all filters, the confidence with which the null hypothesis could be rejected was less than 50%, so there is no statistical significance to the difference in fit parameters, in the sense that Tully-Fisher lines fitted to the Ursa Major galaxies represent the "true" trend among the LSB galaxies about as well as lines fitted to the LSB galaxies directly. We also tested for a shift in the Tully-Fisher zero point between the LSB and Ursa Major samples by fitting a line to the LSB galaxies but forcing the slope to be the same as that derived from the fit to the Ursa Major sample. In all such cases, the differences between the Ursa Major and LSB zero point were smaller than their uncertainties.

TABLE 2

TULLY-FISHER CORRELATION COEFFICIENTS

| Sample | *B* | | *R* | | *I* | |
|---|---|---|---|---|---|---|
| | *r* | *s* | *r* | *s* | *r* | *s* |
| LSB (complete) | −0.38 | −0.35 | −0.33 | −0.19 | −0.83 | −0.84 |
| LSB (restricted) | −0.55 | −0.35 | −0.51 | −0.40 | ... | ... |
| Ursa Major | −0.94 | −0.87 | −0.97 | −0.89 | −0.97 | −0.90 |
| Coma | −0.90 | −0.90 | ... | ... | −0.99 | −0.99 |

NOTE.—*r* denotes the Pearson linear correlation coefficient, and *s* denotes the Spearman rank correlation coefficient.

TABLE 3

TULLY-FISHER FIT PARAMETERS

| Sample/ Filter | Forward Fit $a$ | Forward Fit $b$ | Forward Fit $\sigma$ | Double Regression Fit $a$ | Double Regression Fit $b$ | Double Regression Fit $\sigma$ |
|---|---|---|---|---|---|---|
| LSB (restricted)[a] | | | | | | |
| *B* | −3.52±0.17 | 20.56±0.43 | 0.701 | −10.74±2.06 | 38.10±5.02 | 1.178 |
| *R* | −3.59±0.22 | 19.83±0.53 | 0.713 | −13.18±2.94 | 42.88±7.07 | 1.326 |
| *I* | −6.85±0.22 | 27.35±0.54 | 0.667 | −9.84±1.76 | 34.69±4.31 | 0.792 |
| Ursa Major[b] | | | | | | |
| *B* | −6.36±0.04 | 27.59±0.09 | 0.385 | −7.14±0.50 | 29.46±1.22 | 0.407 |
| *R* | −7.35±0.02 | 28.95±0.06 | 0.327 | −7.85±0.42 | 30.15±1.00 | 0.338 |
| *I* | −7.75±0.02 | 29.41±0.06 | 0.321 | −8.21±0.41 | 30.51±0.99 | 0.331 |
| Coma[c] | | | | | | |
| *B* | −3.14±0.40 | 13.58±0.04 | 0.185 | ... | ... | ... |
| *I* | −5.65±0.20 | 12.29±0.10 | 0.100 | ... | ... | ... |

[a] Fits to the LSB galaxies were of the form mag = $a \times \log w + b$.

[b] Parameters reported here differ slightly from those reported by Pierce & Tully 1988 because three galaxies included in their fit were excluded here for having inclinations $i < 45°$. Fits were of the form mag = $a \times \log w + b$.

[c] Parameters for fits to the Coma sample in *I* are those reported by Bernstein et al. 1994. The fit in *B* was performed using magnitudes reported by Fukugita et al. 1991. In both filters, the fit was of the form mag = $a \times (\log w - 2.602) + b$.

NOTE.—The Forward fits are standard least-squares fits that minimize residuals in luminosity. The Double Regression fits simultaneously minimize residuals in both profile width and luminosity. In all cases, $a$ denotes the slope of the fitted line, $b$ denotes the intercept, and $\sigma$ denotes the rms error of the fit.

The slopes derived for the Coma galaxies in *I* by Bernstein et al. (1994) and in *B* by us from the magnitudes of Fukugita et al. (1991) are lower than any of the slopes derived from the Ursa Major sample and lower than the double-regression slopes derived from the LSB sample. There is no obvious reason why the Tully-Fisher relation for the Coma set should be so different from that of the other two. One possible explanation is the different redshifts of the Coma and Ursa samples. The Coma galaxies have considerably higher recessional velocities than those in the Ursa Major cluster, and claims have previously been made for a decrease in the Tully-Fisher slope with increasing redshift, as summarized by Djorgovski, De Carvalho, & Han (1988). However, the LSB galaxies cover a very broad range of recessional velocities that overlaps the velocities of both the Ursa Major and Coma samples, and yet their slopes are statistically indistinguishable from those of the Ursa Major set. Another possibility may be cluster membership. As Bernstein et al. (1994) note, all the galaxies in their Coma sample are probably in free expansion and not bound to the Coma Cluster; the Ursa Major galaxies selected by Pierce & Tully (1988) are almost certainly bound members of that cluster. The LSB galaxies are field galaxies that come from all around the celestial equator, but in the luminosity-profile width plane they resemble the Ursa Major Cluster galaxies more than the field galaxies of the Coma sample, so it is difficult to ascribe the slope difference to cluster membership. A third property that distinguishes the Coma sample is the range of profile widths represented there. The Coma sample extends to higher profile widths than do either the Ursa Major or LSB samples, and it does not have any galaxies with profile widths as low as the lowest width members of the other two. Some authors, including Aaronson & Mould (1983), Aaronson et al. (1986), and Mould, Han, & Bothun (1989) have presented evidence of nonlinearity in the Tully-Fisher relation. However, the slope difference between the Ursa Major and Coma samples is more severe than any previously claimed curvature of the Tully-Fisher relation at high profile widths. Also, in the region of profile width where the Coma and LSB samples overlap, most of the LSB galaxies lie well below the trend of the Coma sample, thus suggesting that the difference is a shift of both the slope and zero point of the line and not simply a curvature at higher profile widths. Further investigation is needed to determine why the Tully-Fisher slopes of these samples are so different.

### 3.3. *Scatter in the LSB Luminosity–Profile Width Relation*

Examination of the error budget demonstrates that the LSB galaxies exhibit a large intrinsic scatter around the Tully-Fisher trend. First, we have conservatively assumed a 0.1 mag error in the LSB total magnitudes, based on the comparison of *B*-band frames taken of the same galaxies on different nights and with different CCDs. The internal uncertainties for any single measurement, which include the effects of the extrapolation to total magnitudes, are considerably smaller than this, but the external deviations among measurements of the same galaxy on different nights are typically ~0.08–0.1 mag, due in part to the large effect of a slight error in estimating the sky brightness. When all or most of a galaxy's area has flux levels less than 10% that of the sky, a very small error in determining the sky results in a large error in the galaxy's total magnitude. Our procedure for estimating the sky levels in four different parts of the image allows us to estimate the possible sky level errors that could result from residual flat-fielding errors. These remaining flat-fielding errors are typically ~0.3%, and never larger than 1.0%. The change in magnitude that would result from a sky error of a few tenths of a percent varies with the size

of the galaxy on the frame, but it typically is 0.05–0.07 mag. Combining this potential sky error in quadrature with the internal uncertainties yields a total error of 0.08–0.1 mag, which is consistent with the external derivations for those galaxies with multiple observations.

Second, we have assumed a conservative error of 15 km $s^{-1}$ in the profile width of LSB galaxies with high S/N H I profiles (S/N > 20), and we scaled this number up with decreasing S/N. We also assumed an uncertainty of 5° in the inclinations, or 0.06 in ellipticity. Again, this assumed uncertainty is larger than the internal errors in the ellipticity of any one galaxy, but it reflects the potentially large systematic effects of a small error in the sky estimate. The resulting uncertainties in edge-on log $W_{rc}$ of log $W_c$ values have both a mean and a median value of 0.047, which imply typical uncertainties in the luminosities of $B \simeq 0.32$ mag, $R \simeq 0.37$ mag, and $I \simeq 0.38$ mag using the slopes derived from the Ursa Major fits. Adding these values in quadrature to the assumed 0.1 mag photometric uncertainty yields total measurement uncertainties for the LSB galaxies of $B \simeq 0.34$ mag, $R \simeq 0.38$ mag, and $I \simeq 0.39$ mag.

As seen in Table 3, the rms deviations of the LSB galaxies from their forward-fit Tully-Fisher relations are $B \simeq 0.70$ mag, $R \simeq 0.71$ mag, and $I \simeq 0.67$ mag. Substracting the total measurement uncertainties in quadrature yields estimates of the intrinsic scatter as $B \simeq 0.61$ mag, $R \simeq 0.60$ mag, and $I \simeq 0.54$ mag, which are quite large despite the very conservative estimates of the measurement uncertainties. In contrast, Bernstein et al. (1994) found that their data on the Coma sample were consistent with *no* intrinsic scatter in $I$, and Pierce & Tully (1988) found their Ursa Major data to be consistent with an intrinsic scatter of only 0.1 mag in $R$ and $I$ and 0.15 mag in $B$.

## 4. DISCUSSION

To the extent that the Tully-Fisher relation reveals trends in the $M/L$ ratios of spiral galaxies, our data on the LSB galaxies are consistent with the conclusion that LSB field spirals in general have similar $M/L$ ratios to the spirals in the Ursa Major cluster, as we have found no significant difference between the relations for the two samples. There is apparently a significant difference between the Tully-Fisher relations of the LSB spirals and those of the field spirals in the vicinity of the Coma Cluster, but there is also a difference between the Tully-Fisher parameters and hence the $M/L$ ratios of the Coma and Ursa Major samples. As noted above, there is no clear reason why the Coma sample of Bernstein et al. (1994) should be so different from the other two. If the environment has anything to do with the rotation speed or luminosity of a spiral galaxy as suggested by Rubin, Whitmore, & Ford (1988) and Whitmore, Forbes, & Rubin (1988), it would be natural to expect the LSB galaxies, which are drawn from the general field, to more closely resemble another set of field galaxies than a sample drawn from a bound cluster, but instead the converse seems to hold.

As noted above, the LSB galaxies exhibit a large intrinsic scatter (0.61 mag in $B$, 0.60 mag in $R$, and 0.54 mag in $I$) around the baseline Tully-Fisher relation established by the Ursa Major sample. We first considered whether this intrinsic scatter could be produced by peculiar velocities. The mean radial velocity of the LSB sample is 7625 km $s^{-1}$, with a range of $2648 \leq v_{rad} \leq 23{,}528$ km $s^{-1}$. The largest peculiar velocities reported to date are $\sim$600 km $s^{-1}$, e.g., Lauer & Postman (1994). Peculiar velocities this large would imply a mean fractional uncertainty in the redshift distances of 0.072, which in turn translates into a magnitude uncertainty of about 0.15 mag. Subtracting this worst-case estimate in quadrature still leaves intrinsic scatters of 0.59 mag in $B$, 0.58 mag in $R$, and 0.52 mag in $I$. The real contribution of peculiar velocities is likely to be even less than this estimate. Thus most if not all of the intrinsic scatter must be due to real variations in the properties of the LSB galaxies themselves.

### 4.1. *Intrinsic Scatter and Half-Light Radius*

We next investigated the relationship between the Tully-Fisher residuals and the physical size of the LSB galaxies. Figure 3 shows this relation, with size represented by the half-light radii of the galaxies in kpc assuming $H_0 = 100$ km $s^{-1}$ $Mpc^{-1}$; the sense of the residuals is that galaxies that are underluminous with respect to the Tully-Fisher trend line have positive residuals. We used our double regression fits to the Ursa Major sample to define the trend line for calculating the

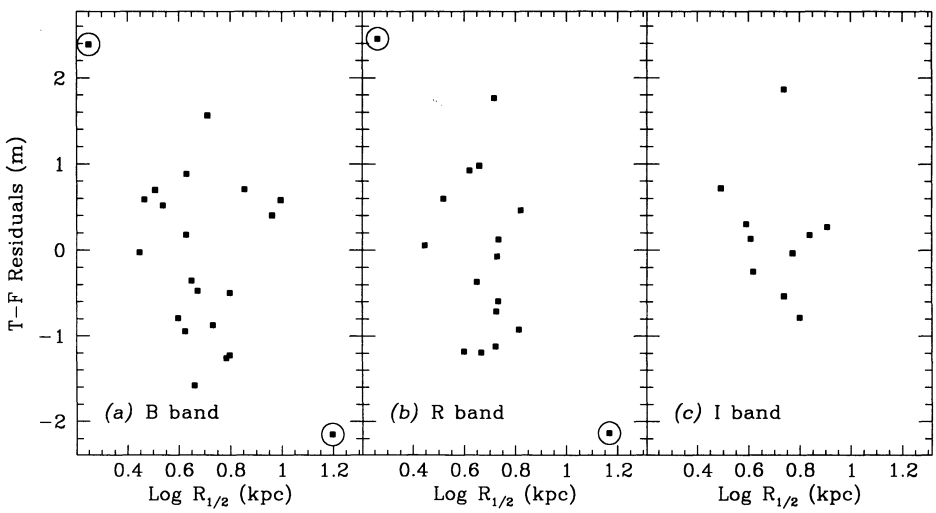


FIG. 3.—Residuals of the LSB spiral galaxies from our Tully-Fisher double-regression fits to the Ursa Major comparison sample, as a function of half-light radius. $R_{1/2}$ is in kiloparsecs, assuming $H_0 = 100$ km $s^{-1}$ $Mpc^{-1}$. The sense of the residuals is that a positive residual indicates a galaxy luminosity lower than predicted. Open circles mark the LSB galaxies excluded from the "restricted" sample because of their radii.

residuals. To quantify this relation, we have computed parametric and nonparametric correlation coefficients, quoted here as (Pearson linear correlation coefficient; Spearman rank correlation coefficient). Using the full sample of LSB galaxies in each filter, the coefficients are $B$: ($-0.49$; $-0.33$), $R$: ($-0.64$; $-0.41$), and $I$: ($-0.17$; $-0.35$). These coefficients suggest a modest trend for small galaxies to be underluminous and large galaxies to be overluminous with reference to the Tully-Fisher trend line, but this suggestion must be treated very cautiously. It is apparent from Figure 3 that the "trend" is mostly due to two galaxies, the smallest (0918−0028) and the largest (1226+0105). These two galaxies are observable only in the spring, and thus were not observed in $I$. When these two galaxies are excluded from the $B$ and $R$ samples, the correlation coefficients drop precipitously to $B$: ($-0.04$; $-0.10$) and $R$: ($-0.14$; $-0.14$). Thus the restricted sample (i.e., the sample without these two galaxies) shows no statistical relation between physical size and deviation from the Tully-Fisher trend.

It is intriguing that the two galaxies that are the most extreme outliers in physical size are also the most extreme outliers from the Tully-Fisher trend line. The galaxy with the largest half-light radius is LSB 1226+0105, which was described in detail by Sprayberry et al. (1993). It is a member of the giant, gas-rich class of LSB spiral galaxies typified by Malin 1. For illustration, we have also plotted the position of Malin 1 on Figures 1 and 2, using data reported by Bothun et al. (1987) and Impey & Bothun (1989). We note that there is some uncertainty about the position of Malin 1. Bothun et al. (1987) were able to measure the surface brightness profile only to 1.5 scale lengths from the center, so a large extrapolation to total magnitude was required (about 0.9 mag). Also, Impey & Bothun (1989) estimated an inclination $i \approx 45°$ largely from circumstantial arguments and noted that the inclination was highly uncertain. At its nominal values of luminosity and inclination, Malin 1 is approximately 1.1 mag overluminous, but it has a half-light radius $R_{1/2} > 50$ kpc and would therefore be well off the scale of Figure 3. If the inclination of Malin 1 were as low as 30°, its position in Figure 1 would shift horizontally to $\log W_{rc} = 2.78$ and its overluminosity would decrease to 0.35 mag. Malin 2, as reported by Bothun et al. (1990), is also a member of this class, but it has an inclination $i < 45°$ and so was not plotted here. Because so much of the luminosity of these giant disks lies in regions of very LSB, use of an isophotal magnitude system suitable for higher surface brightness galaxies would reduce the measured luminosities for the LSB galaxies substantially.

The location of these two giant disks in the luminosity–profile width plane leads to an interesting conundrum. In one sense, it is reasonable that their large sizes and low densities should cause them to lie above the trend. Since the rotation velocity is related to enclosed mass and radius as $v^2 \propto GM(r)/r$, $v$ should go down as $r$ increases or $M$ decreases. On the other, hand the slow rotation speeds and large radii should also imply a very long baryonic cooling time and hence very slow star formation in such disks, as predicted by Hoffman, Silk, & Wyse (1992). These considerations would suggest that the luminosities of these disks should be low, implying that they should fall closer to or even below the general Tully-Fisher trend. The conundrum is that these disks have very high total stellar contents despite their anemic luminosity densities, large radii, and long cooling timescales. Further investigation of the star formation processes and stellar populations of these disks are clearly needed to resolve this riddle.

### 4.2. *Intrinsic Scatter and Galaxy Evolution*

We also explored the relation between residuals from the Tully-Fisher trend and gas richness. Figure 4 shows the comparison of residuals versus the distance-independent ratio of H I mass to luminosity. The residuals were computed in the same manner as for Figure 3. There is some weak relationship between residuals and gas richness apparent in Figure 4. Again, we measured both parametric and nonparametric correlations, which are reported as (Pearson linear correlation coefficient; Spearman rank correlation coefficient). The strength of the correlations for the full samples of LSB galaxies are $B$: (0.37; 0.32), $R$: (0.35; 0.43), and $I$: (0.31; 0.30). In this comparison, excluding the two galaxies with outlier radii (0918−0028 and 1226+0105) improves the correlation coefficients to $B$: (0.58; 0.51), and $R$: (0.64; 0.66). The improvements in both $B$ and $R$ are significant at about the 1 $\sigma$ level. As before, the sense of the residuals is that underluminous galaxies have positive residuals, so the positive correlation coefficients here imply that increasing gas richness is somewhat associated with more severe underluminosity. This association implies that the large intrinsic scatter of the LSB galaxies around the Tully-Fisher trend line may be related to their evolutionary state, in that the underluminous galaxies tend to be that way because they have not yet processed much of their gas into stars. It should be noted that luminosity enters into both sides of this correlation. If a galaxy's luminosity is underestimated, both its Tully-Fisher residual and its gas richness will increase, thus artificially inflating the correlation coefficient. However, as noted in § 3.3, the rms of the residuals is larger than the combined measurement errors and very much larger than the measurement errors in the luminosity alone. Even if all the residuals were reduced by a quadrature subtraction of the luminosity uncertainty, the correlation coefficient would not change significantly.

To explore further the issue of evolution, we also examined the relation between H I mass ($M_{\rm H\,I}$) and profile width. Figure 5 shows this relation, with the corresponding relations for the Ursa Major and Coma samples also. Gas masses for the Ursa Major sample are from the survey of Fisher & Tully (1981), and those for the Coma sample are from the references cited by Bernstein et al. (1994). Estimates of $M_{\rm H\,I}$ assume $H_0 = 100$ km s$^{-1}$ Mpc$^{-1}$. Correlation coefficients for the four samples, using the notation (linear correlation coefficient; Spearman rank correlation coefficient) are LSB(complete): (0.36; 0.45), LSB(restricted): (0.64; 0.67), Ursa Major: (0.60; 0.56), and Coma: (0.30; 0.34). The difference in the correlation between the complete LSB sample and the restricted LSB sample is significant at $\sim 1.5$ $\sigma$. Among the LSB galaxies, there are slight differences among the correlations of profile width against $B$, $R$, $I$, and $M_{\rm H\,I}$, but the significance of the differences is $\lesssim 1$ $\sigma$ in all cases. Among the Ursa Major and Coma samples, however, the correlation between $M_{\rm H\,I}$ and profile width is weaker than the correlation between any measure of optical luminosity and profile width, and the differences are all significant at $\geq 3$ $\sigma$. Table 4 show the parameters of forward fits to the $M_{\rm H\,I}$–profile width relation for the restricted LSB, Ursa Major, and Coma samples. The fit for the restricted sample of LSB galaxies has an intercept that differs substantially from that of the Ursa Major sample, even though the slopes are comparable. The LSB galaxies are clearly offset toward higher H I masses, even though there was no apparent offset in luminosity in the optical Tully-Fisher relations (compare Fig. 5*a* with Fig. 1). The Ursa Major galaxies generally have large angular sizes, so

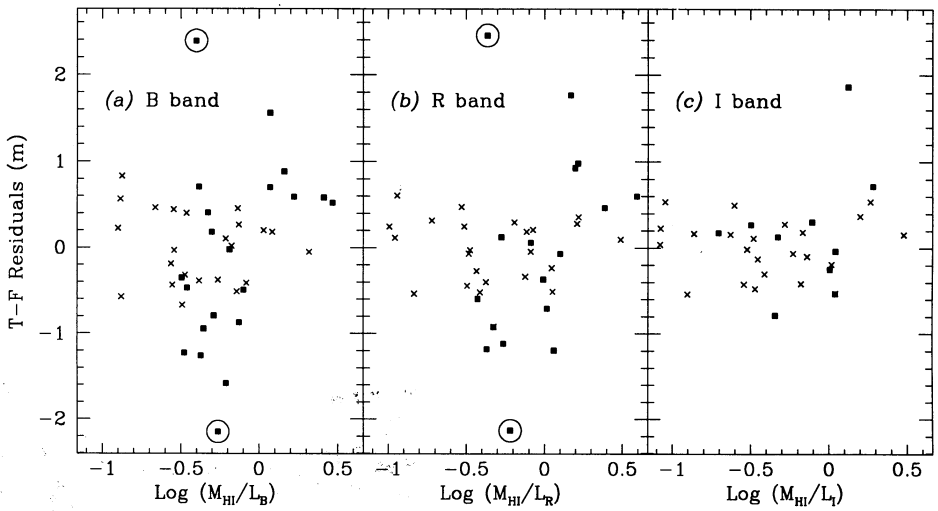


FIG. 4.—Residuals of the LSB spiral galaxies (*dark squares*) and the Ursa Major comparison galaxies (*crosses*) from the double-regression fits to the Ursa Major galaxies, as a function of gas richness. The sense of the residuals is that a positive residual indicates a galaxy luminosity lower than predicted. Open circles mark the LSB galaxies excluded from the "restricted" sample because of their radii.

it is possible that their H I masses are underestimated due to partial resolution by the telescope beam. However, Fisher & Tully (1981) estimated this correction for all the galaxies detected in their survey, and the average correction for these Ursa Major galaxies is 11%. The offset in H I mass between the LSB and Ursa Major samples is 0.75 dex, or about a factor of 5, so it is highly unlikely that beam size effects could be responsible for any significant part of the offset.

Thus, gas mass is as strongly related to rotation speed as is optical luminosity for the LSB galaxies, but the same does not hold for either the Ursa Major or Coma samples. This difference suggests that atomic gas may be a more significant component of total mass among LSB galaxies than for more visible spirals. Thus, LSB galaxies may be well described as unevolved, with considerable raw material still available for processing into stars. This finding is consistent with previous work by McGaugh & Bothun (1994) who found field LSB galaxies to be generally bluer than more visible galaxies and argued that the most likely cause was slow, continuous star formation. Furthermore, the mostly unsuccessful efforts by Schombert et al. (1990) (no detections out of 19 observations) and Knezek (1993) (three detections out of 17 observations) to detect molecular gas in LSB galaxies suggest that star formation in LSB galaxies generally does not occur in the giant molecular clouds seen in more visible spirals.

With this in mind, we examined our results for evidence that differences in stellar populations between LSB and HSB galaxies could account for the large differences in Tully-Fisher scatter. Figure 6 shows the residuals in $B$, $R$, and $I$ plotted against $B-R$ and $B-I$. As can be seen there, the $R$ and $I$ residuals are uncorrelated with color for either the LSB or Ursa Major galaxies; the parametric and nonparametric correlation coefficients are $R$: (0.19; 0.25) and $I$: (0.19; 0.31) for the restricted LSB sample, and $R$: (0.37; 0.32) and $I$: (0.20; 0.20) for the Ursa Major sample. However, $B$ residuals are modestly correlated with color in both galaxy samples; the coefficients for the $B$ versus $B-R$ correlation are restricted LSB: (0.40; 0.42) and Ursa Major: (0.59; 0.56), and the coefficients for the $B$ versus $B-I$ correlation are LSB: (0.59; 0.66) and Ursa Major: (0.59; 0.59). The sense of these correlations is that increasing redness of color is weakly associated with more severe underluminosity. Figure 7 shows the $B-R$ color as a function of

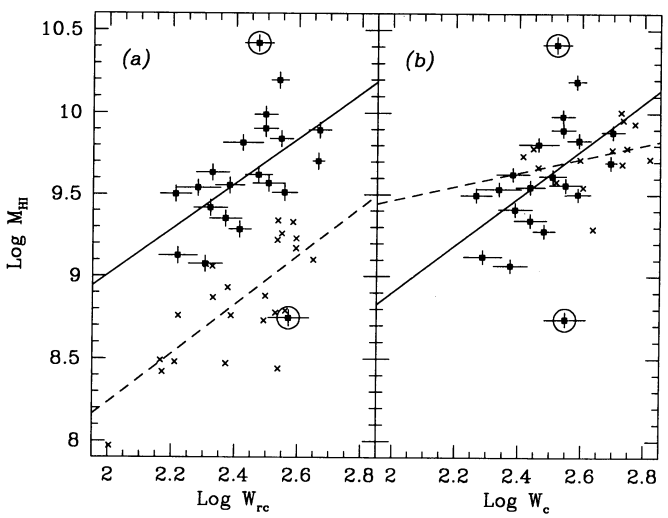


FIG. 5.—log $M_{\rm H\,I}$ as a function of profile width (the "21 cm Tully-Fisher relation"). $M_{\rm H\,I}$ is in units of solar mass, assuming $H_0 = 100$ km s$^{-1}$ Mpc$^{-1}$. (*a*) Squares represent LSB galaxies, and crosses represent the Ursa Major galaxies. (*b*) Squares represent the LSB galaxies, and crosses represent the Coma galaxies. Solid lines show the forward fits to the LSB galaxies, and dashed lines show the forward fits to the comparison galaxies. Open circles mark the LSB galaxies excluded from the "restricted" sample because of their radii.

TABLE 4

$M_{\rm H\,I}$ VERSUS LOG W FIT PARAMETERS

| Sample | *a* | *b* | *σ* |
|---|---|---|---|
| LSB (complete) | 1.06±0.07 | 7.02±0.18 | 0.347 |
| LSB (restricted) | 1.38±0.08 | 6.25±0.18 | 0.217 |
| Ursa Major | 1.19±0.05 | 6.39±0.13 | 0.269 |
| Coma | 0.43±0.09 | 8.61±0.24 | 0.164 |

NOTE.—All fits here are forward fits, i.e., standard least-squares fits that minimize residuals in $M_{\rm H\,I}$. *a* denotes the slope and *b* denotes the intercept, as $M_{\rm H\,I} = a \times \log {\rm W} + b$.

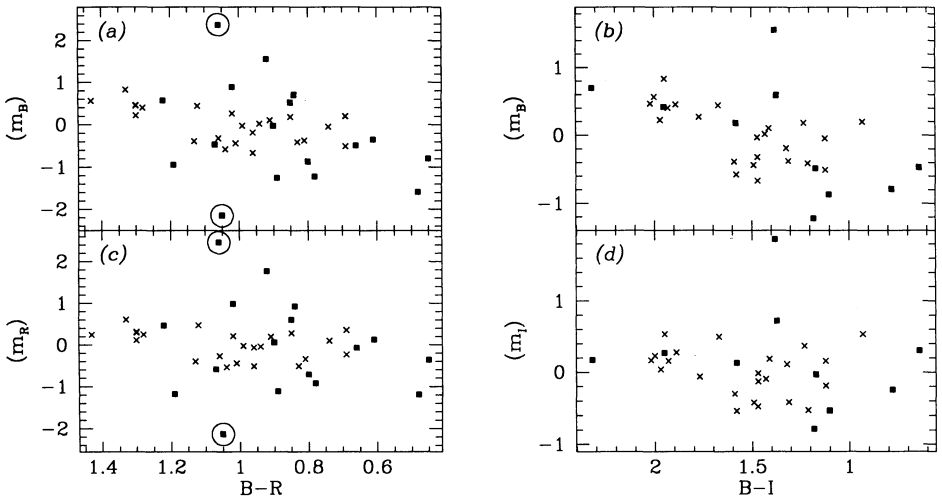


FIG. 6.—Residuals of the LSB spiral galaxies (*filled squares*) and the Ursa Major comparison galaxies (*crosses*) from the double-regression fits to the Ursa Major galaxies, as a function of galaxy total color. (*a*) *B* residuals vs. $B-R$; (*b*) *B* residuals vs. $B-I$; (*c*) *R* residuals vs. $B-R$; (*d*) *I* residuals vs. $B-I$. The sense of the residuals is that a positive residual indicates a galaxy luminosity lower than predicted. Open circles mark the LSB galaxies excluded from the "restricted" sample because of their radii.

profile width for the LSB and Ursa Major samples, with best-fit straight lines drawn to highlight the general trend in each sample. Both samples get redder with increasing profile width, but the mean color for the LSB sample of $B-R = 0.87$ is 0.16 mag bluer than the mean color for the Ursa Major sample of $B-R = 1.03$ (the standard error of the mean for each sample is 0.03 mag). Pierce & Tully (1992) noted a similar difference in $B-I$; they found the Ursa Major galaxies to be about 0.25 mag redder on average than their six local calibrator galaxies. These differences suggest that the stellar populations found in the Ursa Major sample are different, possibly due to a deficiency of gas in the galaxies inhabiting the dense cluster environment. However, the similarity and weakness of correlations of residuals against color for the LSB and Ursa Major samples suggest that any differences in stellar populations between the two samples probably do not account for the differences in their scatters in the Tully-Fisher plane.

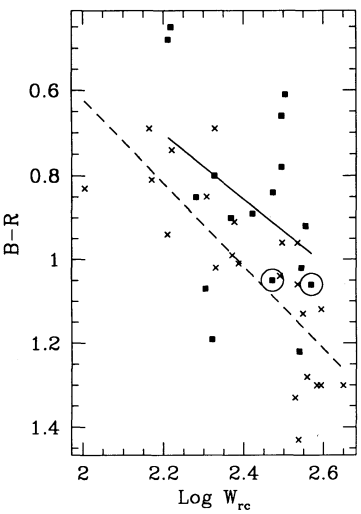


FIG. 7.—$B-R$ total galaxy color as a function of H I profile width for the LSB spiral galaxies (*dark squares*) and the Ursa Major comparison sample (*crosses*). Open circles mark the LSB galaxies excluded from the "restricted" sample because of their radii. The solid line shows the best-fit straight line for the LSB galaxies, and the dashed line shows the best-fit straight line for the Ursa Major galaxies.

## 5. CONCLUSIONS

We have reported total magnitudes and H I profile widths for a sample of field LSB spiral galaxies and have compared these results to those of more visible galaxies using the familiar Tuly-Fisher relation. We find that the field LSB spirals generally follow the same Tully-Fisher relation as more visible galaxies in the Ursa Major cluster, albeit with a considerably higher scatter. This similarity suggests that the LSB spirals examined here generally have similar total $M/L$ ratios to those of the Ursa Major spirals, although the higher scatter suggests that the range of $M/L$ ratios may be larger among LSB galaxies. We also find that both the LSB and Ursa Major samples fall along substantially different Tully-Fisher relations from that defined by a sample of field galaxies in the direction of the Coma Cluster, but we can find no convincing explanation for the difference.

Among the LSB galaxies, the weak trend of Tully-Fisher residuals to increase with increasing gas richness suggests that differences in evolutionary status among LSB galaxies may account for some part of the higher scatter. Differences in luminosity–profile width correlations among the *B*, *R*, and *I* filters suggest that differences in stellar populations may also play a role. Further, a relation between $M_{HI}$ and profile width that, while modest, is stronger than the *B* Tully-Fisher relation suggests that atomic gas may be a larger fraction of total mass for LSB galaxies than for the Ursa Major comparison sample. Finally, the two giant Malin 1–class LSB spirals for which suitable data are available are both substantially overluminous for their rotation speeds, a fact that is difficult to reconcile with their low-luminosity densities and presumed long cooling timescales.

We thank M. Pierce and H.-W. Rix for helpful discussions. As always, we are grateful for the skilled and good-humored assistance of the telescope operators and staff at the Arecibo Observatory and the Steward Observatory Kitt Peak Station. This work was supported in part by National Science Foundation grant AST 90-03158. D. S. was supported by a National Science Foundation Graduate Research Fellowship. G. B. was supported by the Bart J. Bok Fellowship from Steward Observatory.

## REFERENCES


Aaronson, M., Bothun, G., Mould, J., Huchra, J., Schommer, R. A., & Cornell, M. E. 1986, ApJ, 302, 536
Aaronson, M., Huchra, J., & Mould, J. 1979, ApJ, 229, 1
Aaronson, M., & Mould, J. 1983, ApJ, 265, 1
Bernstein, G. M., Guhathakurta, P., Raychaudhury, S., Giovanelli, R., Haynes, M. P., Herter, T., & Vogt, N. P. 1994, AJ, 107, 1962
Binggeli, B., Sandage, A., & Tammann, G. A. 1985, AJ, 90, 1681
Bothun, G. D., Impey, C. D., & Malin, D. F. 1991, ApJ, 376, 404
Bothun, G. D., Impey, C. D., Malin, D. F., & Mould, J. R. 1987, AJ, 94, 23
Bothun, G. D., & Mould J. R. 1987, ApJ, 313, 629
Bothun, G. D., Schombert, J. M., Impey, C. D., & Schneider, S. E. 1990, ApJ, 360, 427
Burstein, D., & Heiles, C. 1982, AJ, 87, 1165
Christian, C. A., Adams, M., Barnes, J. V., Butcher, H., Hayes, D. S., Mould, J. R., & Siegel, M. 1985, PASP, 97, 363
Coleman, G. D., Wu, C.-C., & Weedman, D. W. 1980, ApJS, 43, 393
Disney, M. J. 1976, Nature, 263, 573
Djorgovski, S., De Carvalho, R., & Han, M.-S. 1988, in The Extragalactic Distance Scale: Proc. ASP 100th Anniversary Symp., ed S. van den Bergh & C. J. Pritchet (ASP Conf. Ser. 4), 329
Fisher, J. R., & Tully, R. B. 1981, ApJS, 47, 139
Fukugita, M., Okamura, S., Tarusawa, K., Rood, H. J., & Williams, B. A. 1991, ApJ, 376, 8
Hoffman, Y., Silk, J., & Wyse, R. F. G. 1992, ApJ, 388, L13
Holmberg, E. 1958, Med. Lunds Astron. Obs., II, No. 136
Impey, C., & Bothun, G. 1989, ApJ, 341, 89
Impey, C., Bothun, G., & Malin, D. 1988, ApJ, 330, 634
Impey, C. D., Sprayberry, D., Irwin, M. J., & Bothun, G. D. 1994, in preparation
Irwin, M. J., Davies, J. I., Disney, M. J., & Phillipps, S. 1990, MNRAS, 245, 289
Kent, S. M. 1986, AJ, 91, 1301
———. 1987, AJ, 93, 816
Knezek, P. M. 1993, Ph.D. thesis, Univ. Massachusetts
Landolt, A. U. 1992, AJ, 104, 340
Lauer, T. R., & Postman, M. 1994, ApJ, 425, 418
McGaugh, S. S., & Bothun, G. D. 1994, AJ, 107, 530
Miller, R. W., & MacGillivray, H. T. 1994, BAAS, 25, 1292
Mould, J., Han, M.-S., & Bothun, G. 1989, ApJ, 347, 112
Odewahn, S. C., Bryja, C., & Humphreys, R. M. 1992, PASP, 104, 553
Pierce, M. J., & Tully, R. B. 1988, ApJ, 330, 579
———. 1992, ApJ, 387, 47
Rubin, V. C., Whitmore, B. C., & Ford, W. K., Jr. 1988, ApJ, 333, 522
Schombert, J. M., & Bothun, G. D. 1988, AJ, 95, 1389
Schombert, J. M., Bothun, G. D., Impey, C. D., & Mundy, L. G. 1990, AJ, 100, 1523
Schombert, J. M., Bothun, G. D., Schneider, S. E., & McGaugh, S. S. 1992, AJ, 103, 1107
Sprayberry, D., Impey, C. D., Irwin, M. J., McMahon, R. G., & Bothun, G. D. 1993, ApJ, 417, 114
Tully, R. B., & Fisher, J. R. 1977, A&A, 54, 661
Tully, R. B., & Fouqué, P. 1985, ApJS, 58, 67
Whitmore, B. C., Forbes, D. A., & Rubin, V. C. 1988, ApJ, 333, 542